Matrix Completion Techniques For Anomaly Detection in Network Attacks

A Thesis
Presented to
Department of Statistical Science
Duke University

James C. Wu

May 2018

Approved for the
Bachelor of Science in Statistical Science

Peter D. Hoff

Jerry P. Reiter

Galen Reeves

Mine Cetinkaya-Rundel, DUS

Acknowledgements

I thank my advisor, Professor Peter Hoff, and the Director of Undergraduate Studies, Professor Mine Cetinkaya-Rundel, for their guidance in this project. I also thank Duke University's Statistics Department for supervising this project and the Office of Information Technology for providing the dataset. Most of all I thank my parents for their continued unwavering support in all my endeavors.

Table of Contents

Abstract

The goal of this paper is to identify novel methods for detecting anomalies in network IP data. The data is comprised of four continuous features (source bytes, destination bytes, source packets, destination packets) divided by their respective source port and destination port combinations. Thus, the data is represented as a 3-dimensional tensor $T \in \mathbb{R}^{m \times n \times 4}$, where m is the number of source ports, n is the number of destination ports, and 4 is the number of continuous features. Each cell in T, t_{ijk} stores the mean of the observations of continuous feature k between source port at index i and destination port at index j. This paper proposes three techniques for generating means to fill in the missing cells in T, thereby completing the tensor, so as to provide reasonable estimates for new observations between every possible port combination. In the context of anomaly detection, new observations between ports that do not align closely with their corresponding estimate in T are considered anomalies. The first technique uses a low-rank singular value decomposition algorithm for completing individual matrix slices of the tensor. The second defines a statistical model for the values in T and uses a Bayesian Gibbs Sampling Procedure to simulate missing values in individual matrix slices of T. Finally, the third approach extends the first and second approaches to completing the tensor all at once, rather than with completing individual matrices.

The goal of this paper is to identify novel methods for detecting anomalies in network IP data. The data is comprised of four continuous features (source bytes, destination bytes, source packets, destination packets) divided by their respective source port and destination port combinations. Thus, the data is represented as a 3-dimensional tensor $T \in \mathbb{R}^{m \times n \times 4}$, where m is the number of source ports, n is the number of destination ports, and 4 is the number of continuous features. Each cell in T, t_{ijk} stores the mean of the observations of continuous feature k between source port at index i and destination port at index j. This paper proposes three techniques for generating means to fill in the missing cells in T, thereby completing the tensor, so as to provide reasonable estimates for new observations between every possible port combination. In the context of anomaly detection, new observations between ports that do not align closely with their corresponding estimate in T are considered anomalies. The first technique uses a low-rank singular value decomposition algorithm for completing individual matrix slices of the tensor. The second defines a statistical model for the values in T and uses a Bayesian Gibbs Sampling Procedure to simulate missing values in individual matrix slices of T. Finally, the third approach extends the first and second approaches to completing the tensor all at once, rather than with completing individual matrices.

Chapter 1

Introduction

1.1 Anomaly Detection

Anomaly detection is used to identify unusual patterns or observations that do not conform to expected behavior in a dataset. Anomalies can be broadly categorized into three categories:

Point anomalies: A single instance of data is anomalous if it's too far off from the rest. For example detecting credit card fraud based on a single spending spree that represents the credit card being stolen and used.

Contextual anomalies: The abnormality is context specific. This type of anomaly is common in time-series data. For instance, high spending on food and gifts every day during the holiday season is normal, but may be considered unusual otherwise.

Collective anomalies: A set of data observations that when collectively assessed helps in detecting anomalies. For instance, repeated pings from a certain IP address to a port connection on a hosted network may be classified as a port scanner, which often preludes a network attack.

1.2 Network Attacks

Network security is becoming increasingly relevant as the flow of data, bandwith of transactions, and user dependency on hosted networks increase. As entire networks grow in nodes and complexity, attackers gain easier entry points of access to the network. The most benign of attackers attempt to shutdown networks (e.g. causing a website to shutdown with repeated pings to its server), while more malicious attempts involve hijacking the server to publish the attacker's own content or stealing unsecured data from the server, thus compromising the privacy of the network's users.

Attackers follow a specific three step strategy when gathering intelligence on a network, the most important component of which is scanning. Network scanning is a procedure for identifying active hosts on a network, the attacker uses it to find information about the specific IP addresses that can be accessed over the Internet, their target's operating systems, system architecture, and the services running on each node/computer in the network. Scanning procedures, such as ping sweeps and port scans, return information about which IP addresses map to live hosts that are active on the Internet and what services they offer. Another scanning method, inverse mapping, returns information about what IP addresses do not map to live hosts; this enables an attacker to make assumptions about viable addresses.

All three of these scanning methods leave digital signatures in the networks they evaluate because they apply specific pings that are then stored in the network logs. Most scanners use a specific combination of bytes, packets, flags (in TCP protocol), and ports in a sequence of pings to a network. Identifying a scanner's often many IP addresses from the set of pings available in the network's logs is thus an anomaly detection problem. In particular, because the data is unlabeled, meaning it is unclear which observations are actually scanners and which are just standard user behavior, unsupervised approaches are necessary for tackling the problem.

1.3 Network Dataset

This particular dataset is from Duke University's Office of Information Technology (OIT), and it covers all observations in their network traffic during a five minute period in February 2017.

1.3.1 Features

The networks dataset contains 13 features, 8 categorical and 5 continuous, and the observations are unlabeled (not specified whether they are considered a scanner). The 13 features are:

Continuous:

- StartTime (Start Time): the time when the observation is logged
- SrcBytes (Source Bytes): the total number of bytes sent in the observation
- SrcPkts (Source Packets): the number of packets sent in the observation
- DstBytes (Destination Bytes): the total number of bytes received in the observation
- DstPkts (Destination Packets): the number of packets received in the observation Note, the destination packets and bytes features do not have the same values as their source counterparts because the connections are compressed and decompressed into different forms and byte sizes when sent. For instance, it is

possible for the number of destination packets to be larger than source packets. It is also possible for information to be lost during the connection.

Categorical:

- Flgs (connection flag): flow state flags seen in transaction between the two addresses
- Proto (network protocol): specifies the rules used for information exchange via network addresses. Transmission Control Protocol (TCP) uses a set of rules to exchange messages with other Internet points at the information packet level, and Internet Protocol (IP) uses a set of rules to send and receive messages at the Internet address level.
- SrcAddr (Source Address): the IP address of the connection's source
- DstAddr (Destination Address): the IP address of the connection's destination
- Sport (Source Port): the network port number of the connection's source. A port numbers identifies the specific process to which a network message is forwarded when it arrives at a server.
- Dport (Destination Port): the network port number of the connection's destination
- Dir (direction): the direction of the connection
- State (connection state): a categorical assessment of the current phase in the transaction when the timestamp is recorded

Note, the addresses have been anonymized for security reasons.

1.3.2 Argus

Argus is the open source network security tool applied to network transactions that collects the data for the features. The Argus wiki and the OIT manual provides key insights into the structure and nature of the data. Specifically, the sessions are clustered together by address, so the pytes and packets values are accumulative over a set duration and each session has its own start time but does not have a tracked end time. There exist 2-4 million connections on average every 5 minutes. Furthermore the protocol in this dataset is always gathered from TCP protocol and the direction will always be to the right (i.e. Source to Destination). This information supports dropping proto, StartTime, and Direction from the dataset for future analysis because they do not present any information regarding whether an observation can be considered an anomaly. Furthermore, the State feature may not be reliable because Argus occasionally resets the state data statistics during monitoring.

1.3.3 Status Quo Solution

OIT's current solution for detecting scanners relies on specific domain knowledge gathered from diagnostics programs and data analysis completed on previous data.

They prevent scanners by blocking IP addresses that fit certain rules they have constructed to run on every network transaction as it occurs. The specific checks in these rules are private for security reasons, but they belong to the nature of evaluating the size of transactions, repeated connections between particular ports, many pings from the same address, and combinations of these particular behaviors.

While this solution presents a methodical way for banning IP addresses and its method of rule checking is essentially removing what OIT considers outliers for network transactions-any observation that does not fit within the constraints specified by the rules is classified as an outlier and its source IP is blocked-it is inflexible, prone to detecting false negatives, and fails to detect observations that may be within the parameter constraints of the rules but are anomalous with respect to other parameters or parameter constraints.

1.4 Problem Formulation

Preliminary data analysis signaled that there may exist trends between different port combinations. For instance, a particular source and destination port may frequently contain large byte transactions in their connections. Devising a systematic way to identify these combinations may present outliers that can be further investigated for scanner behavior.

This approach to the anomaly detection problem reduces the dataset to the values of the four continuous features, SrcBytes, SrcPkts, DstBytes, DstPkts, observed across different source port and destination port combinations. The data can be represented as a 3-dimensional tensor $T \in \mathbb{R}^{m \times n \times 4}$ where m represents the number of source ports, n represents the number of destination ports, and 4 accounts for the four continuous features in the dataset. Each cell, t_{ijk}, contains the mean of all the observations observed between the source port at index i and destination port at index j. In the cases where the combination of i and j is not observed in the dataset, t_{ijk} is considered missing (NA). Note, the data is collected in a way where either all four continuous features are observed, or none are observed, i.e. a missing cell, t_{ij1} indicates $t_{ij2}, t_{ij3} and t_{ij4}$ are also missing.

The goal of this paper is to devise and assess strategies for calculating a reasonable estimate for the missing cells in T to create the completed tensor $T' \in \mathbb{R}^{m \times n \times 4}$. As new observations are observed for combinations of source ports at index i and destination ports at index j, the t'_{ijk} values can be interpreted as an approximation for the expected behavior for that particular port combination. Observations with continuous features that are a certain threshold away from t'_{ijk} may be marked as anomalies and investigated further.

1.5 Introduction of Methods

Chapters 3,4, and 5 discuss three methods for completing the tensor T. The first two techniques slice T into four matrices divided by the four continuous features: $Y^{(1)}, Y^{(2)}, Y^{(3)}, Y^{(4)} \in \mathbb{R}^{m \times n}$. Because both techniques apply to each matrix separately, the techniques will refer to a general matrix Y, which represents any of $Y^{(1)}, Y^{(2)}, Y^{(3)}, Y^{(4)}$. Each $Y^{(k)}$ has missingness because not every source port interacts with every destination port. Chapter three considers an iterative approach using an alternating least squares technique and the best low-rank approximation of Y to repeatedly calculate estimates for the missing values of the singular value decomposition of Y. While the approach does not consider the variable sample sizes and variances for each port combination, essentially treating each cell as a scalar value rather than a mean of observations, it is the fastest technique of the three and provides reasonable performance metrics. Chapter four shores up the weaknesses of chapter three by defining an additive statistical model that accounts for the variable sample sizes and variances of the observations in each port combination. This model is generalized to a weighted least squares problem, and a Bayesian approach is used to create a Gibbs Sampler to iteratively simulate the row factors and column factors with their respective variances of the model. Each approach is validated on simulated data where the ground truth is known to verify correctness before being applied to the actual networks dataset. Finally, chapter five proposes a tensor completion technique that simulates cells in T without slicing the tensor. This approach allows considers correlation and collinearity between the different continuous features and relies on the PARAFAC tensor decomposition (as opposed to the two-dimensional matrix singular value decomposition).

Chapter 2

Modeling Port Relationships

The following properties of T inform the matrix and tensor completion strategies in chapters 3, 4, and 5.

2.1 Missingness

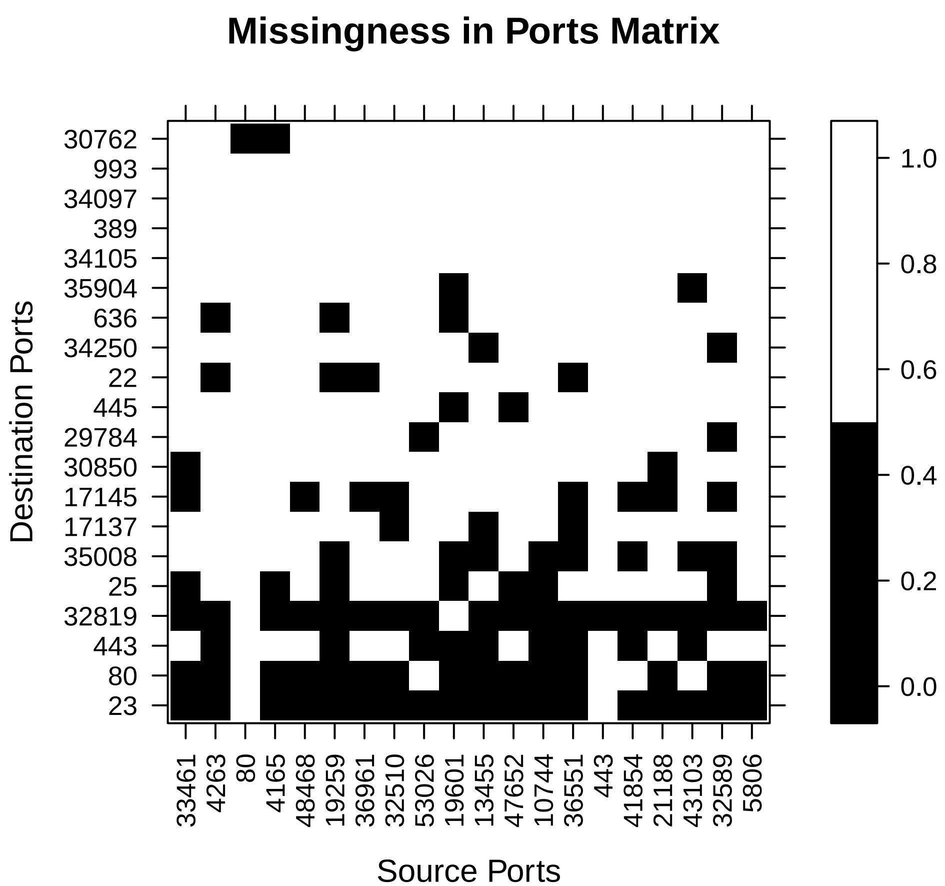

The above matrix represents the missingness in the port combinations for pairings of the top 20 most used source ports and destination ports. The black cells represent missingness; of the 400 cells in the matrix, 295 (73.75%) of cells are missing observations. This single matrix slice can be extrapolated to missingness in ports throughout the entire tensor because the dataset is collected in a way such that either all four continuous features are observed, or none are observed. It is important to note that missingness is not uniform across source and destination port combinations. In the event that an entire row or column of port combinations is missing, the port at that respective index will need to be discarded from the simulation procedure because all three techniques depend on the row and column effects when simulating a value for a missing cell.

2.2 Row and Column Properties

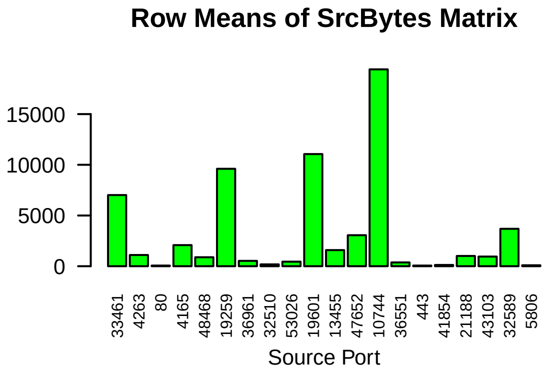

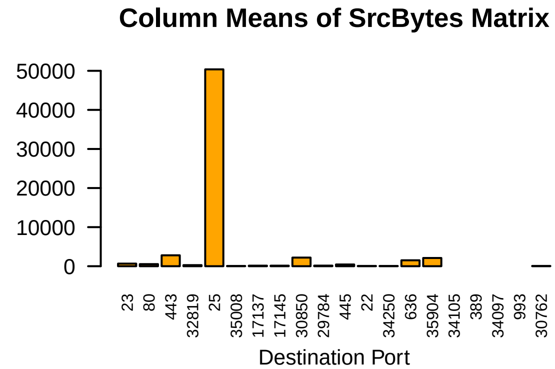

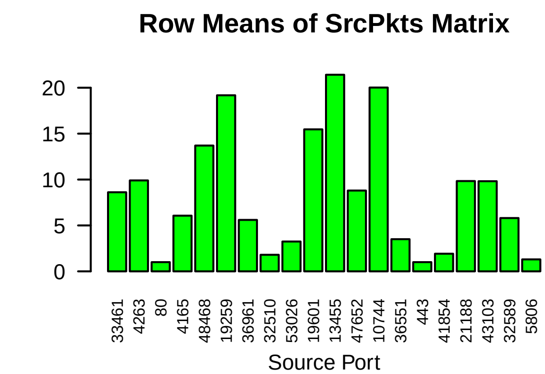

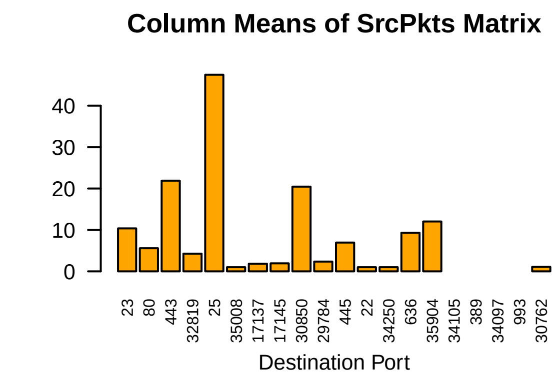

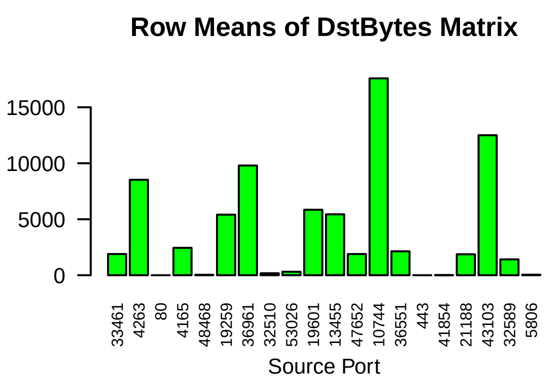

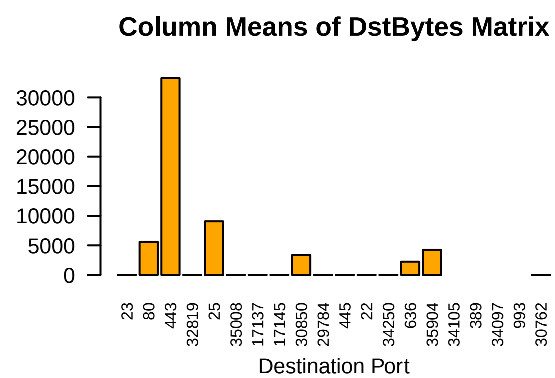

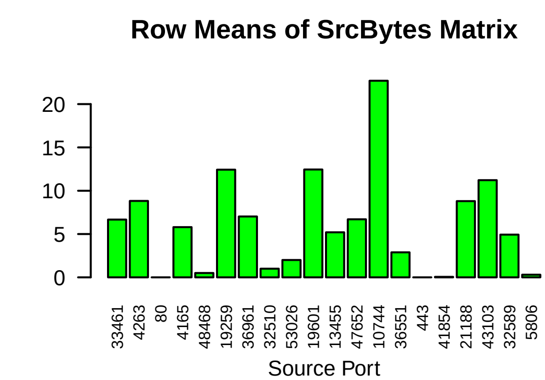

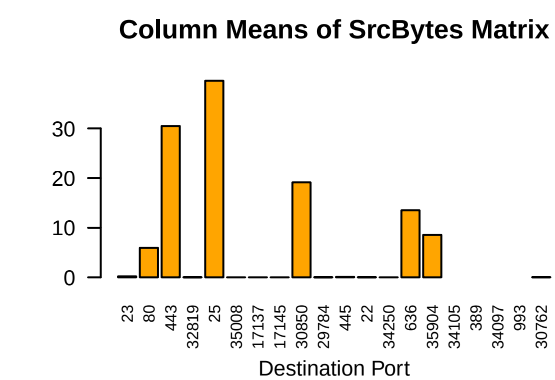

The bar plots above represent the row and column means of the continuous features for each slice of the tensor. These row means and column means inform simulation techniques for the missing cells within those respective rows and columns. There exist clear outliers in the means for certain rows and columns. This outlier behavior is undoubtedly caused by outliers existing within the cells in that particular row or column. These outliers exist because each cell represents the mean of all observations that occured within a particular port combination, regardless of sample size (i.e. some cells may have a few large observations, resulting in a large mean that skews the cell's row and column mean). Thus, cells that only have a few observed observations have a disproportionately large effect on their respective row and column mean.

These outliers may cause problems with simulating missing values in that row or column because the outliers will have a disproportionately large effect on the simulated value than the other observations, which are more close to the median in the missing value's row or column. This behavior suggests that the completion techniques that take into account variances among the row and column means and the number of samples observed for each port combination will result in more accurate estimations for the missing port combinations.

2.3 Port Connections

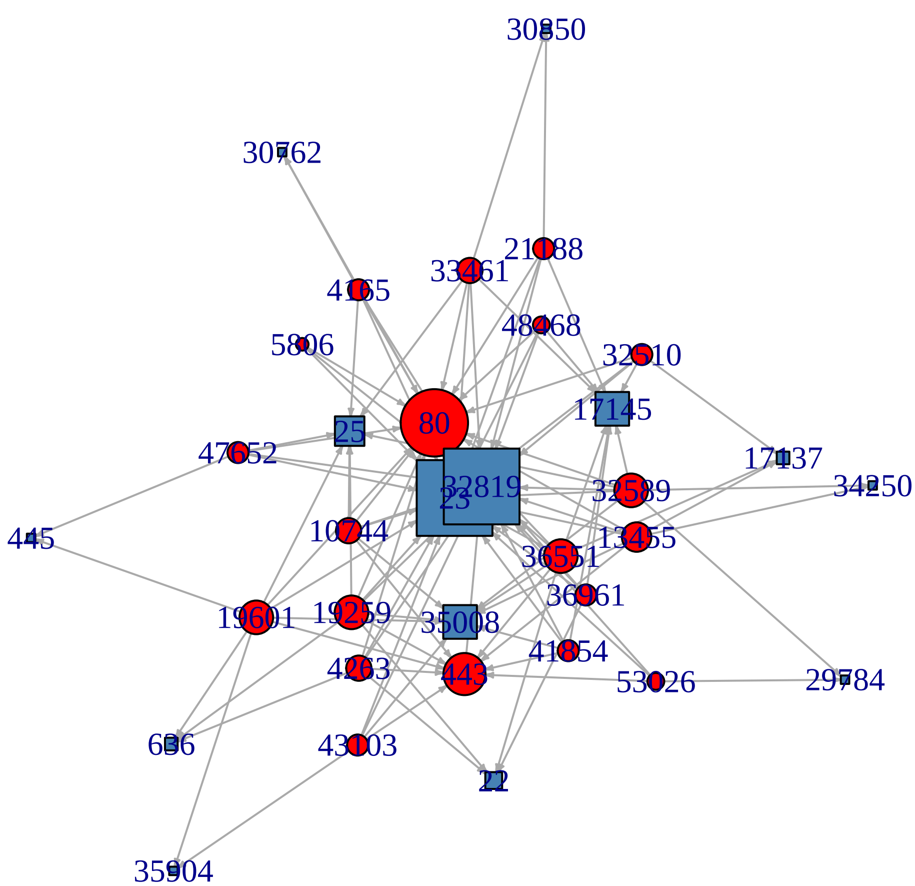

The above ports network graph displays the pairings between the top twenty source ports (red circles) and the top destination ports (blue squares). When a square and circle are connected it represents that there exist observations for this particular port combination in the dataset. The size of each node reflects the number of paired observations that were observed using that particular port. Clearly, not every source port is paired with a destination port and vice versa (not every node is connected to every other node). These missing combinations reflect missing cells in the T tensor, and consequently they correspond to the combinations that require values to be simulated.

2.4 Varied Sample Sizes

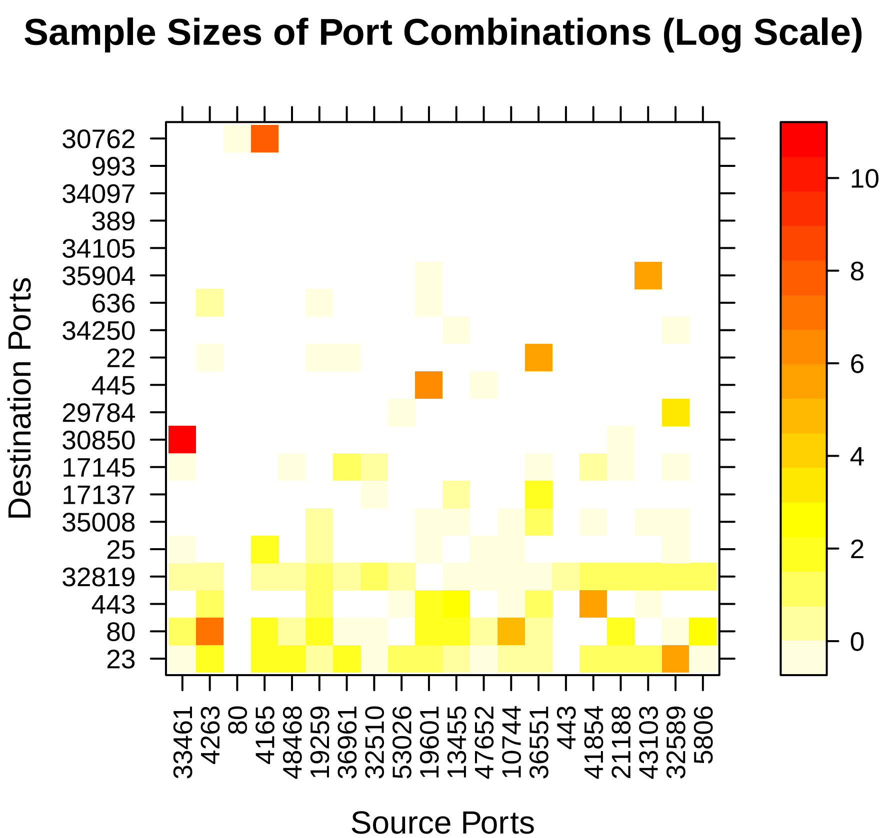

Finally, to better visualize the sample sizes first displayed in the network graph, the above heat plot represents the sample sizes for each source-destination port combination on a log scale for clarity. It is again clear there are certain combinations that have many observations (range of 35000 on the original scale), while most of the observations are 0, indicating no observations were observed and the corresponding cell in T is missing, or near 0, indicating few observations were observed. The large variation in sample sizes again suggests a simulation technique that accounts for sample size of a missing cell's related row and column cells is necessary.

2.5 Correlations

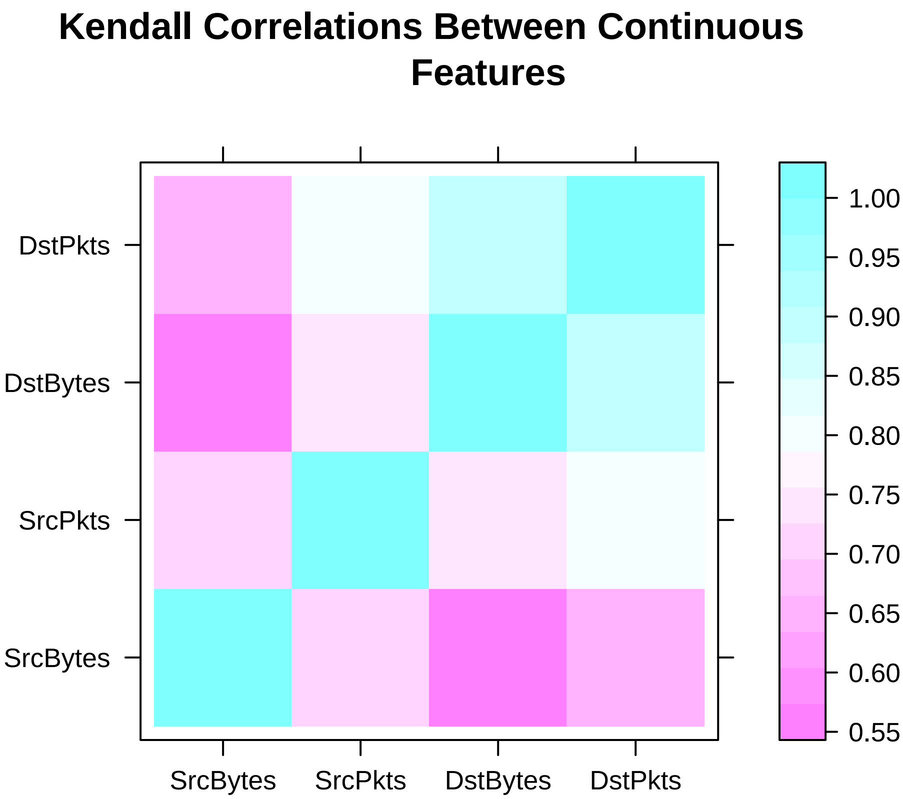

The matrix above describes the Kendall rank correlations (commonly referred to as Kendall's tau coeffıcent) between the four continuous features in the dataset. Intuitively, the Kendall correlation between two features will be high when observations have a similar rank (i.e. relative position label of observations within the variable: 1st, 2nd, 3rd, etc.) between the two variables, and low when observations have a dissimilar rank between the two variables. The range of correlations is [-1, 1]. Kendall correlation was selected as a measure because it evaluates ranks between observations, as opposed to Pearson, which is more susceptible to outliers in the dataset (large byte and packet observations in the continuous features skewed the Pearson measures).

It is clear there exist strong correlations between the four continuous features, DstBytes and DstPkts in particular. This behavior suggests a technique that simulates estimates for the missing cells with all four features considered at once (i.e. a technique that simulates the entire tensor as a whole rather than in slices) will also be valuable.

Chapter 3

Alternating Least Squares Applied to Two Dimensional Matrices

This approach determines the best low-rank approximation for Y using the Eckart-Young-Mirsky Theorem to repeatedly generate the orthonormal matrices U and V of the singular value decomposition of Y ($Y = UDV^T$) in an alternating pattern. The technique is proven to correctly determine a low rank approximation on simulated matrices where the true rank is known. Once the optimal low rank is determined from the actual dataset the optimal low rank is used in the technique to simulate the estimates for the missing cells of Y. The technique's fit is assessed by comparing the fitted versus the observed values

3.1 Related Work

NEED TO MENTION THAT THERE IS A SIMPLIFIYING ASSUMPTION WHEN CONDUCTING MATRIX COMPLETION THAT THE MATRIX IS LOW RANK, ONE OF MANY APPROACHES TO MATRIX COMPLETION

`https://arxiv.org/abs/1410.2596` `https://www.netflixprize.com/assets/GrandPrize2009_BPC_BigChaos.pdf`

Similar techniques for matrix completion were employed in the Netflix Challenge where top competitor predicted ratings for movies by users that had not watched the movie based on the other ratings in the matrix of users and movies.

3.2 Matrix Completion Algorithm

$F \in \mathbb{R}^{m \times n}$ is a sparse matrix that represents the frequencies of combinations, i.e $F[32242, 12312]$ represents the number of observations for the 32242 12312 port combination $M \in \mathbb{R}^{m \times n}$ represents a boolean matrix of whether the corresponding Y values are missing. $Y[M]$ represents all of the missing values in Y.

The objective is

$$\min_{r} \sum_{i,j:F_{i,j}>0} (y_{i,j} - u_i D v_j^T)^2$$

where $UDV^{(k)T}$ represents the singular value decomposition of Y and r is the low rank approximation for Y. There are multiple steps to the matrix completion process:

3.2.1 ANOVA Initial Imputation

An analysis of variance (ANOVA) imputation is used to fill in the initial values for y_{ij}. This yields an additive model dependent upon the means of the present observations:

$$y_{ij} = a_i + b_j - \mu$$

whereμ is the overall mean of Y, a_i is the row mean, and b_j is column mean of y_{ij}.

3.2.2 Repeated Simulation

The repeated imputation procedure solves $Y^{(s)}[M] = R_r(Y^{(s-1)})[M]$ where $R_r(...)$ is the best rank r approximation for the s-th step. For each step (s) the singular value decomposition decomposes

$$Y^{(s)} = U^{(s)} D^{(s)} V^{T(s)}$$

where D is a diagonal matrix of the singular values, U is the left singular vectors of Y and V is the right singular vectors of Y.

The Eckart-Young-Mirsky Theorem provides the best rank r approximation for the missing values in $Y^{(s+1)}$. Recall $Y[M]$ represents all of the missing values of Y. Applying the EYM theorem:

$$Y^{(s+1)}[M] = (U[,1:r]^{(s)} D[,1:r]^{(s)} V[,1:r]^{T(s)})[M]$$

Where $U[,1:r]$ represents the first r columns of U and the same for D and V.

3.2.3 Convergence Criterion

The Eckart-Young-Mirsky rank approximation step is repeated until the relative difference between $Y^{(s+1)}$ and $Y^{(s)}$ falls below a set threshold, H. The relative difference threshold is expressed:

$$\frac{\|Y^{(s+1)} - Y^{(s)}\|_2}{\|Y^{(s)}\|_2} < H$$

where $\|Y\|_2$ is the Frobenius norm for matrices. The denominator of the expression ensures the convergence criterion is invariate to a scale change in the matrix itself.

3.3 Best Low Rank Approximation

To determine the best low rank for approximating Y, Leave-One-Out Cross Validation (LOOCV) is used to generate prediction errors for each possible rank. LOOCV cycles through the observed values, setting each to NA (missing), and then performing the described matrix completion process. The prediction error is then calculated as some function of the difference between the imputed value and the true value. In this case, the algorithm records root mean square error

$$\sqrt{\frac{\sum(\hat{y}_{ij} - y_{ij})^2}{z}}$$

where z is the number of observations not missing.

3.4 Validation Against Simulated Data

Before applying the algorithm on the real data it is useful to validate the algorithmic approach against simulated data where the true rank is already known.

3.4.1 Simulating a Low Rank Matrix

Taking the Kronecker product of two lower dimension matrices yields a higher dimension matrix with low rank. Explicitly, given matrix $A \in \mathbb{R}^{m\times r}$ and $B \in \mathbb{R}^{r\times n}$, $A \otimes B = C$ where $C \in \mathbb{R}^{m\times n}$ has rank r. Thus, when $r < m, r < n$ the matrix C has an optimal low rank that minimizes the root mean square error from the leave one out cross validation procedure. To add noise to the simulated matrix, C, simply add an error matrix, $E \in \mathbb{R}^{m\times n}$ sampled from a normal distribution.

This procedure provides a computationally efficient way to simulate many random low rank matrices to use as inputs for the validation procedure. In the case of simulated matrices, there are no missing entries, so the leave one out cross validation procedure sequentially removes each cell in the matrix, imputes its value using the rank being investigated, and considers the individual cell error as the difference between the true value and the imputed value. The overall root mean square error for the technique is then calculated with the aggregate each of these individual cell errors.

3.4.2 Approximating Optimal Rank

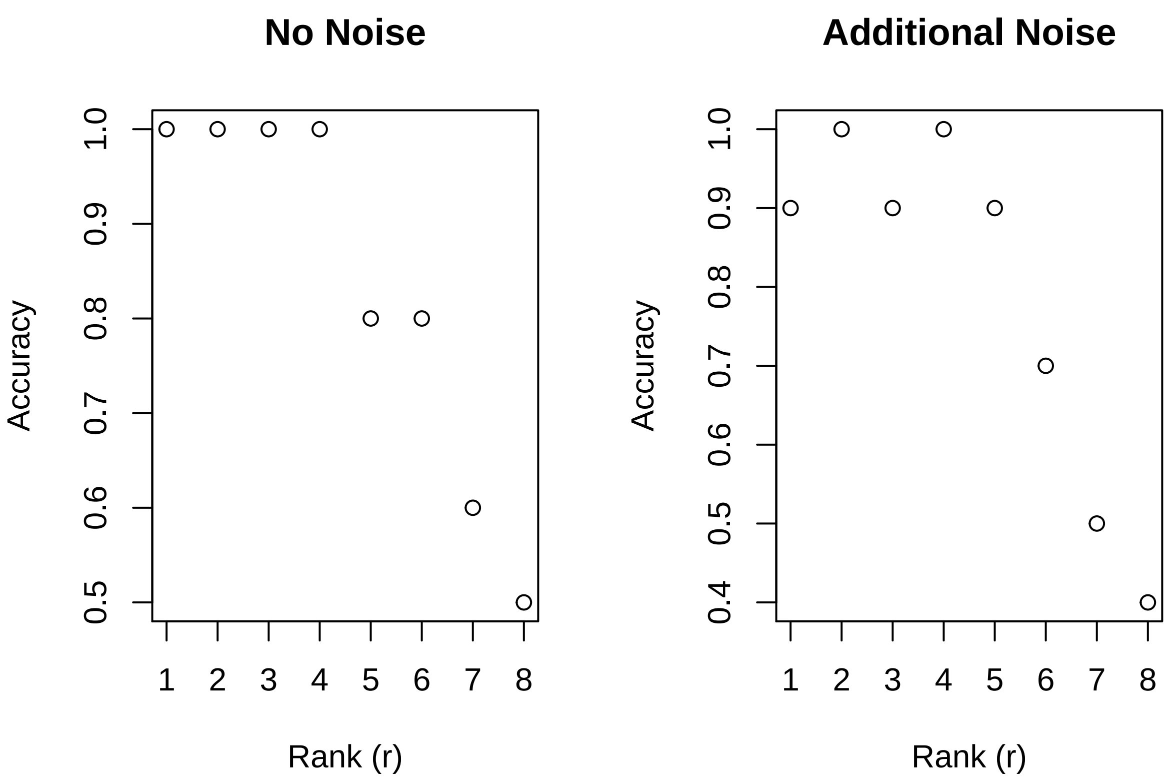

The above plots represent the accuracy of the matrix completion technique for matrices with true rank $r = 1, 2, ...8$. The accuracy is measured by simulating 10 random matrices (dimensions ranging from 74 to 100 values) with low rank of r for each value of r (80 simulated matrices total), and then running the leave one out cross validation procedure described above on the matrix C to generate a root mean square error for each possible rank. The accuracy is the calculated using the number of times the rank with the lowest error matches the true simulated rank divided by 100 (the number of trials with rank r). Note as the true rank becomes larger, the technique performs far worse at determining the true rank. This behavior is due to the fact that LOOCV attempts to find the rank that minimizes the root mean square error, not necessarily the true low rank approximation for a matrix. Higher true ranks tend to give higher out-of-sample validation error, so LOOCV will still select a low rank approximation for simulated matrices that have relatively high true ranks. For instance, a simulated data matrix may have a true rank of 8, but it may also be very close to rank 2, which results in LOOCV selecting rank 2 as the optimal low rank approximation for minimizing error.

Furthermore, when noise is applied to each simulated matrix, C, (through the addition of a noise matrix E), the algorithm tends to perform worse at a majority of the attempted ranks. This is expected because the addition of noise to every cell in the matrix may obscure the true rank from the LOOCV procedure.

3.5 Results on Real Data

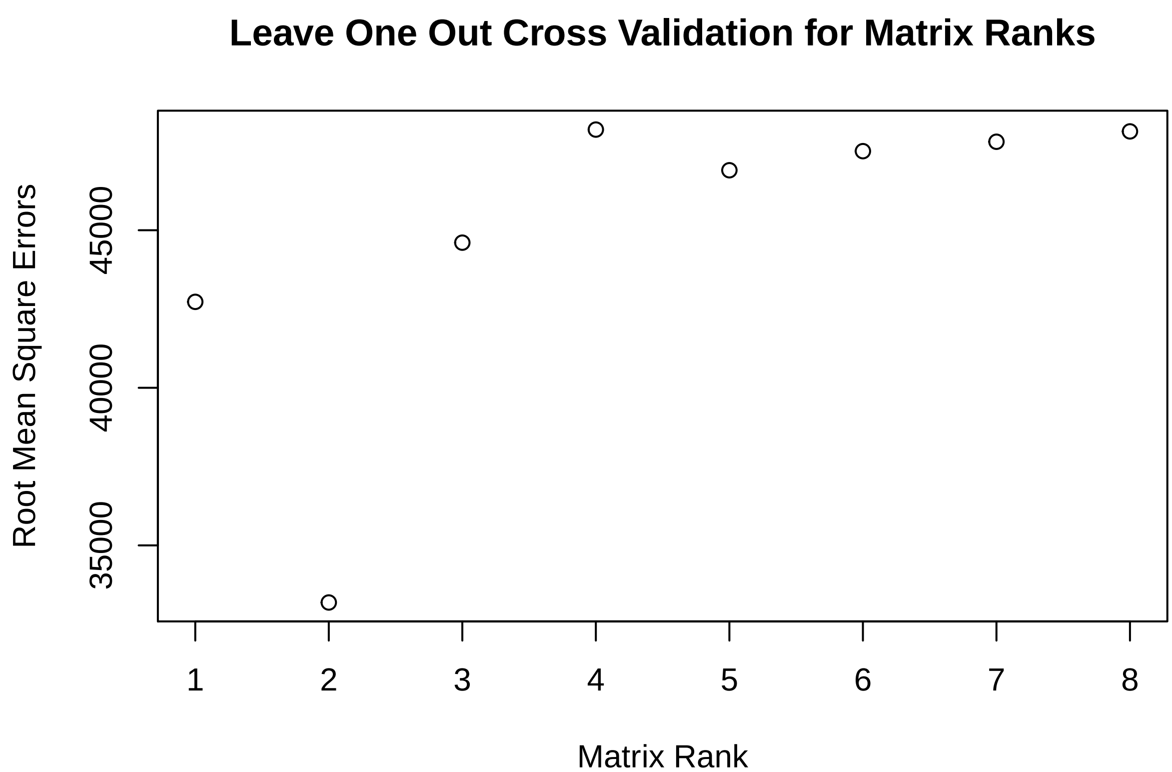

The above plot displays the root mean square errors from the leave one out cross validation process across different rank inputs into the algorithm. It's clear that rank 2 provides the best low-rank approximation for simulating missing values in Y using the alternating least squares algorithm. Thus, the dataset is fitted with the algorithm using rank 2 to simulate the missing values in Y.

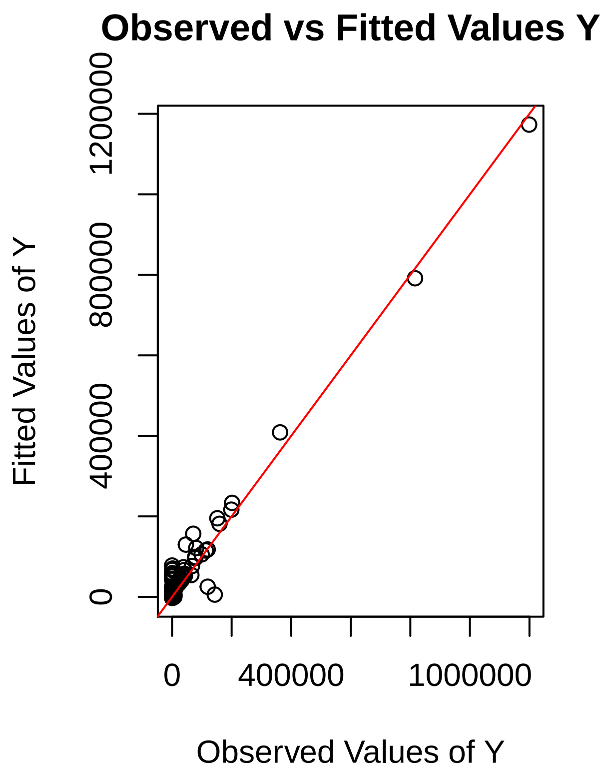

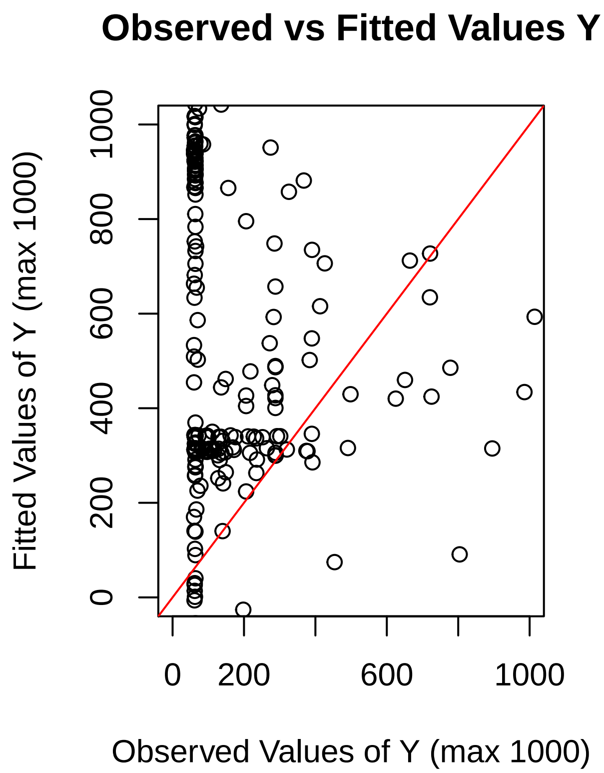

The two plots above display the true values of the Y matrix (i.e. the non-missing values) versus their corresponding fitted values using the alternating least squares algorithm with an input of rank 2. The first plot displays all values and shows a somewhat positive linear trend (an ideal fit of the true values would be a scatter of points following a linear relationship, represented in red). However, several outliers with large true values skew this dataset and cause the plot to appear linear. Closer examination of the true and fitted values smaller than 1000 (the plot on the right) reveals the relationship is far from the linear pattern.

3.5.1 Scale Transformations

The poorly fitted results motivates a consideration of the scale of the data. The present algorithm uses the sample averages of the overall matrix as well as the row and column means when imputing each missing cell value. This reliance upon sample means leads to susceptiblity to outliers. Moreover exploratory data analysis reveals the dataset contains outliers, particularly in the SrcBytes and DstBytes measurements. Because outliers drive the sum of squares for the alternating least squares procedure, the poor fit on the data is unsurprising. Thus, a transformation of features in the dataset may be appropriate for improving the fit of the algorithm.

When a natural logarithm transformation is applied to the raw dataset before any simulation steps are taken, the alternating least squares imputation algorithm yields the following root mean square errors varied by rank.

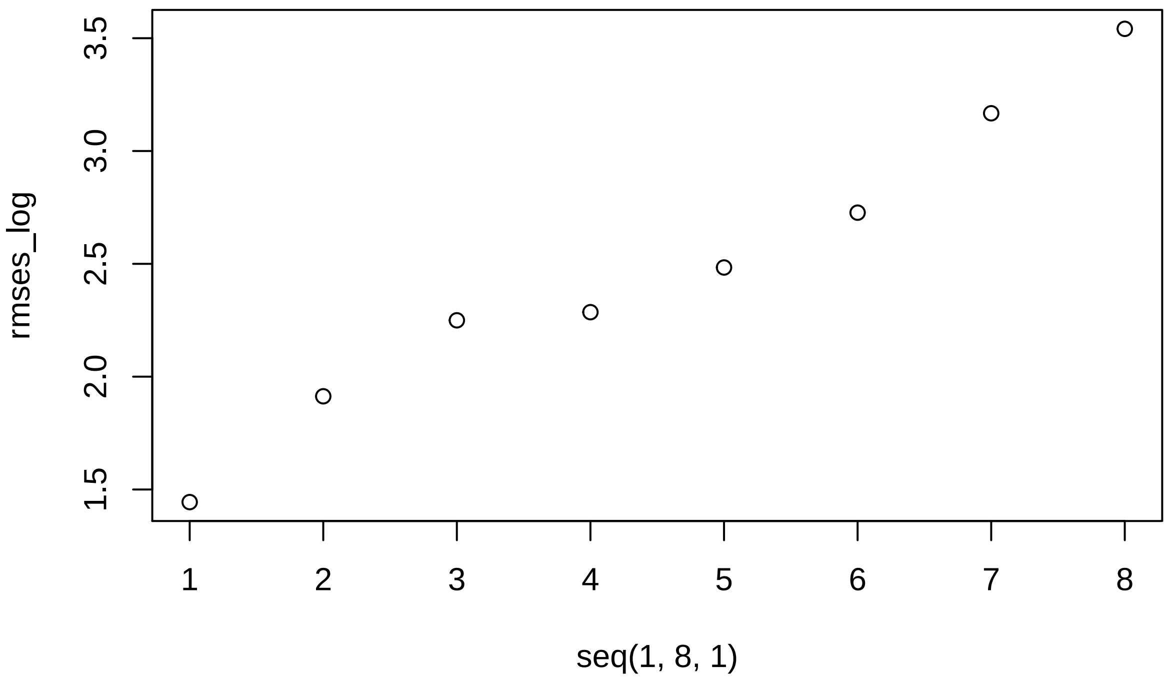

Now the optimal rank from the LOOCV procedure is 1. The algorithm is run on the log transformed dataset with a low rank approximation of 1 and the fitted vereus observed values are again compared.

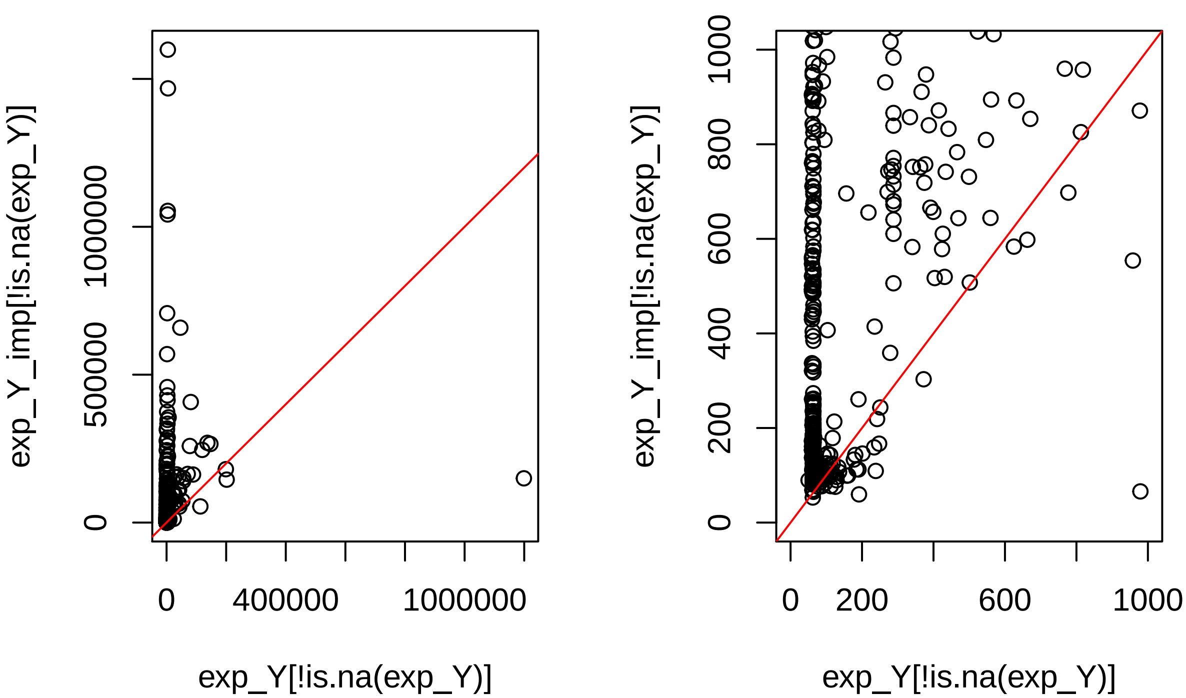

The values above have been retransformed (exponentiated) to the dataset's original scale after the simulation procedure was completed. The fit still appears to be quite poor and there is not much difference between the log transformed output versus the original non-transformed output.

This poor performance may largely be due to the fact the algorithm does not account for the variability in the sample size and variance in the observed interactions for each cell. Unlike the Netflix Competition, in which each cell of the matrix being completed contained only a single user rating of a movie, the matrix in this problem contains the mean of a variable number of observations corresponding to particular port combinations.

Chapter 4

A Bayesian Approach to Two Dimensional Matrix Completion

The previous section's results reflected the need for a completion strategy that accounts for the variability in the number of observations observed for each port combination when imputing that particular combination's cell. The previous technique fails to take into account the differing sample size and variance in each cell's observations, so the algorithm treated each y_{ij} as a single value rather than the mean and variance of a vector of observations. The following section constructs a statistical model that takes the sample size of observations and their variances for each cell into account and repeatedly simulates values for the missing cells using a Gibbs Sampling procedure. The sampling procedure relies upon first building a general model for simulating the row and column facors with their respective standard deviations. After calculating the full conditionals for the parameters of this general model, the overall procedure repeatedly simulates values from these full conditional distributions, alternating between simulating the matrix of row factors and the matrix of column factors along with their respective standard deviations. Note, this technique again slices the tensor into the four separate matrices, $Y^{(1)}, Y^{(2)}, Y^{(3)}, Y^{(4)} \in \mathbb{R}^{m \times n}$ (referred to as Y in general), and the model can be applied to each matrix $Y^{(k)}$ separately.

4.1 Statistical Model for Port Relationships

The following statistical model is defined for the cells in Y:

$$y_{ij} = u_i^T v_j + \frac{\sigma_i \tau_j}{\sqrt{s_{ij}}} \epsilon_{ij}$$

where u_i represents the row factors, v_j represents the column factors, σ_i represents the standard deviation of each row in the matrix, τ_j represents the standard deviations of each column in the matrix, s_{ij} represents the sample size of observations observed for source port i and destination port j, and $\epsilon_{ij} \sim N(0, 1)$. Fixing the j values in the analysis (i.e. v_j and τ_j are known) enables the model to be rewritten in the form of a weighted least squares model for imputing u_i and σ_i. Similarly, when i is fixed, the model can be rewritten to simulate v_j and τ_j. To demonstrate this property, the procedure for simulating u_i and τ_j given known values for v_j and τ_j is described below. The same procedure is possible for v_j and τ_j when u_i and σ_i are known.

4.2 General Model for Simulating Row and Column Factors

Varying $j = 1...n$ the model above yields the following cell values:

$$y_{i1} = u_i^T v_1 + \frac{\sigma_1 \tau_j}{\sqrt{s_{ij}}} \epsilon_{ij}$$

$$...$$

$$y_{in} = u_i^T v_n + \frac{\sigma_1 \tau_j}{\sqrt{s_{ij}}} \epsilon_{ij}$$

Vectorizing all of these equations varied across $j = 1...n$ yields:

$$\vec{y_i} = V u_i + \sigma_i W^{1/2} \vec{\epsilon}$$

where $V \in \mathbb{R}^{n \times r}$ is the matrix of column factors (p is the dimension of the latent factors), and $W \in \mathbb{R}^{n \times n}$ is the diagonal matrix of weights, such that

$$V = \begin{bmatrix} v_1^T - \\ v_2^T - \\ ... \\ v_n^T - \end{bmatrix}, W = \begin{bmatrix} w_1 & & \\ & \ddots & \\ & & w_n \end{bmatrix} = \begin{bmatrix} \frac{\tau_1^2}{s_{11}} & & \\ & \ddots & \\ & & \frac{\tau_n^2}{s_{nn}} \end{bmatrix}$$

Note τ^2 refers to the variance, variance being the square of the standard deviation.

This model can be rewritten in a general form:

$$\vec{y} = X\beta + \sigma W^{1/2} \epsilon$$

where X represents V, β represents u_i and $sigma$ represents σ_i.

This is a modified form of the Generalized Least Squares Model (GLS), which gives a weighted least squares estimate of β, and it is appropriate when the error terms are not independent and identically distributed. Bayesian analysis of this problem provides similar parameter estimates to GLS, and both ordinary least squares and GLS provide unbiased parameter estimates of β with the latter giving estimates with a lower variance because the non-Bayes estimator serves as a limit of the Bayes estimator.

The full conditional distributions of the random variables β and σ^2 (note σ is squared in the model) for this case are described below:

$$\{\beta \mid X, \vec{y}, \sigma^2\} \sim MVN(\beta_n, \Sigma_n)$$

$$\{\sigma^2 \mid X, \vec{y}, \beta\} \sim IG(\frac{\nu_0 + n}{2}, \frac{v_0\sigma_0^2 + SSR_W}{2})$$

where MVN represents the Multivariate Normal Distribution, and IG represents the Inverse Gamma distribution.

$$\begin{cases} \Sigma_n = (X^T W^{-1} X/\sigma^2 + \Sigma_0^{-1})^{-1} \\ \beta_n = \Sigma_n(X^T W^{-1} y/\sigma^2 + \Sigma_0^{-1}\beta_0) \end{cases}$$

$$SSR_W = (y - X\beta)^T W^{-1}(y - X\beta)$$

The remaining variables in the closed form full conditionals come from the parameter's prior distributions, which are defined as follows:

$$\beta \sim MVN(\beta_0, \Sigma_0)$$
$$\sigma^2 \sim IG(\frac{\nu_0}{2}, \frac{v_0}{2}\sigma_0^2)$$

The initial values for the prior distributions are set as: $\beta_0 = 0$, $\Sigma_0 = \gamma^2 I$ where γ^2 is a large number and I is the $m \times n$ identity matrix, $\nu_0 = 2$, $\sigma_0^2 = 1$. This results in a diffuse prior for β that spreads out the density, and a noninformative prior for σ_0^2.

4.2.1 Generalized Gibbs Sampler Function

Following the formulation of the model and the definition of the priors, a general Gibbs Sampler function is created to simulate samples from the full conditional of each parameter in the statistical model, which iteratively creates an approximate value for each cell.

The Gibbs Sampler algorithm progresses as follows:

Let the parameters at step s be:

$\phi^{(s)} = \{\beta^{(s)}, \sigma^{2(s)}\}$

Sample $\beta^{(s+1)} \sim P(\beta \mid X, \vec{y}, \sigma^{2(k)})$

Sample $\sigma^2 \sim P(\sigma^2 \mid X, \vec{y}, \beta^{(s+1)})$

Set $\phi^{(s+1)} = \{\beta^{(s+1)}, \sigma^{2(k+1)}\}$

This Gibbs Sampler serves as a general technique that can be used to simulate both the values of u_i and σ_i or v_j and τ_j depending on the inputs it is given because the formulation of both models are identical; they only differ by the the inputs, X and W, which are calculated, and y which is sliced directly from Y. In the context of the problem, this function can first be called repeatedly to simulate all of the rows in the matrix Y, then called repeatedly with updated inputs to simulate all of the columns of the matrix.

4.2.2 Validation Simulated Data

Before using the general Gibbs sampler function in the overall procedure for simulating missing values in Y, it is necessary to validate the procedure's effectiveness on simulated data where the ground truth is known. As the algorithm runs, it stores a matrix of β vectors and a vector of σ^2 scalars. Thus, if $S = 50$, i.e. the algorithm samples 50 β and 50 σ, the final returned output will be

$$\beta = \begin{bmatrix} \beta_1^T - \\ \beta_2^T - \\ \cdots \\ \beta_{50}^T - \end{bmatrix}, \vec{\sigma^2} = \begin{bmatrix} \sigma_1^2 \\ . \\ . \\ \sigma_{50}^2 \end{bmatrix}$$

Using random sampled values from the normal distribution for X and random sampled values from the exponential distribution for W (exponential distribution is used to ensure Σ_n is positive definite), it is possible to calculate values of $\vec{y}$ using a predefined $\beta*$ and $\sigma*$, which are known as the ground truth values for comparison:

$$\vec{y} = X\beta * + \sigma * W^{1/2}\epsilon$$

This $\vec{y}$, W, and X are used as inputs to the general Gibbs Sampler Function to generate a distribution of β's and a distribution σ^2's. The posterior means of these distributions are then computed and compared to recover the original values, $\beta*$ and $\sigma*$.

In particular, the posterior mean of σ^2 is calculated by taking the mean of the function's output of σ^2. This posterior mean is compared to the original $\sigma*$ used to generate $\vec{y}$. Repeatedly performing this procedure reveals the posterior mean only differs from the ground truth value by 1-2% in almost every single trial.

Recovering the original $\beta*$ provides a much more defined procedure for evaluating the performance of the Gibbs Sampler. First, the Bayes estimator (the posterior mean of generated βs) should be close to the GLS estimator and theoretical results state the GLS estimator serves as a good approximation for the true value. Furthermore, the variance matrix of the GLS estimator around the true value is

$$Var(\hat{\beta}_{GLS}) = \mathbb{E}[(\hat{\beta}_{GLS} - \beta*)(\hat{\beta}_{GLS} - \beta*)^T] = (X^T W^{-1} X/\sigma^2)^{-1}$$

. Thus, after simulating many data sets and solving for the posterior mean estimator, $\hat{\beta}$, the variance of these simulated posterior means, $Var(\hat{\beta})$ should be close to $(X^T W^{-1} X/\sigma^2)^{-1}$. Moreover, the standard errors are calculated

$$SE(\hat{\beta}_{GLS}) = \sqrt{diag((X^T W^{-1} X/\sigma^2)^{-1})}$$

. This provides a nominal 95% confidence interval for which to assess the performance of the model for recovering the original $\beta*$.

4.3 Full Sampling Procedure

The complete Gibbs Sampler for imputing missing values uses the generalized Gibbs Sampler defined above to iteratively simulate missing values for the entire matrix Y. The procedure is described below:

Initialize σ_i for $i = 1...m$ and τ_j for $j = 1...n$ as the overall standard deviation of the $Y^{(k)}$ matrix. Initialize missing values of Y using the ANOVA imputation described in the previous section. Initialize the matrix of row factors $U \in \mathbb{R}^{m\times p}$ and the matrix of column factors $V \in \mathbb{R}^{n\times p}$.

Repeat the following:

1. For $i = 1...m$: Simulate u_i and σ_i using the generalized Gibbs Sampler. For the first iteration of the sampler, set X to the V matrix in the singular value decomposition of Y. For all future iterations, the use the stored V from the pervious iteration as X. For the first iteration, use the initialized τ_j for $j = 1...n$ to calculate the diagonals for the W matrix. For all future iterations use the stored τ_j values from the previous iteratioWn to calculate W. Take the corresponding y_i directly from the Y matrix. Store the resulting sampled u_i's in a matrix U, and the σ_i in a vector, to use for simulating v_j and τ_j.

2. For $j = 1...n$: Simulate v_j and τ_j using the generalized Gibbs Sampler. Use the stored U from the previous step as the X input and use the stored τ_j to calculate the W input. Take the corresponding y_j directly from the Y matrix. Store the resulting sampled v_j's in a matrix V, and the τ_j in a vector, to use for simulating u_i and σ_j.

3. Simulate values for y_{ij} in Y that were missing in the original dataset by sampling from the normal distribution

$$y_{ij} \sim N(u_i^T v_j, \frac{\sigma_i^2 \tau_j^2}{s_{ij}})$$

4.3.1 Selecting the Dimension of Latent Factors

The dimension of the latent factors, p, is used to define the dimension of $\beta \in \mathbb{R}^{p\times 1}$ and consequently defines the dimensions of the row and column factor matrices U and

V. Selecting p is a model selection choice similar to determining the optimal low rank approximation r in the previous section. Once again, Leave One Out Cross Validation may be used to detemine the optimal p given the observed data. In this technique, it is more computationally expensive than the previous technique to perform Leave One Out Cross Validation on the entire dataset, so randomly selecting a set number of observed cells to set to missing for determining p is also valid.

4.3.2 Validation on Simulated Data

Again it is necessary to validate the effectiveness of the overall sampling procedure with simulated data where the ground truth is known. Simulate matrices U and V such that $\Theta = UV^T$ is truly low rank. The same procedure for generating low rank matrices used in the previous chapter can be applied here. Using Θ there are two possible tests for determining the validity of the sampling procedure. First, the simulated data is used to recover the true values for UV^T from the model. This is considered an idealized case for testing the procedure. Second, some cells are set to missing and again the procedure is used to obtain an estimate for UV^T from the model. This output is compared to the previous case's output to evaluate the performance depending on whether the cells have data or do not.

Chapter 5

Future Work: Tensor Completion

Recall the analysis of correlations between the continuous features in T in chapter 2.

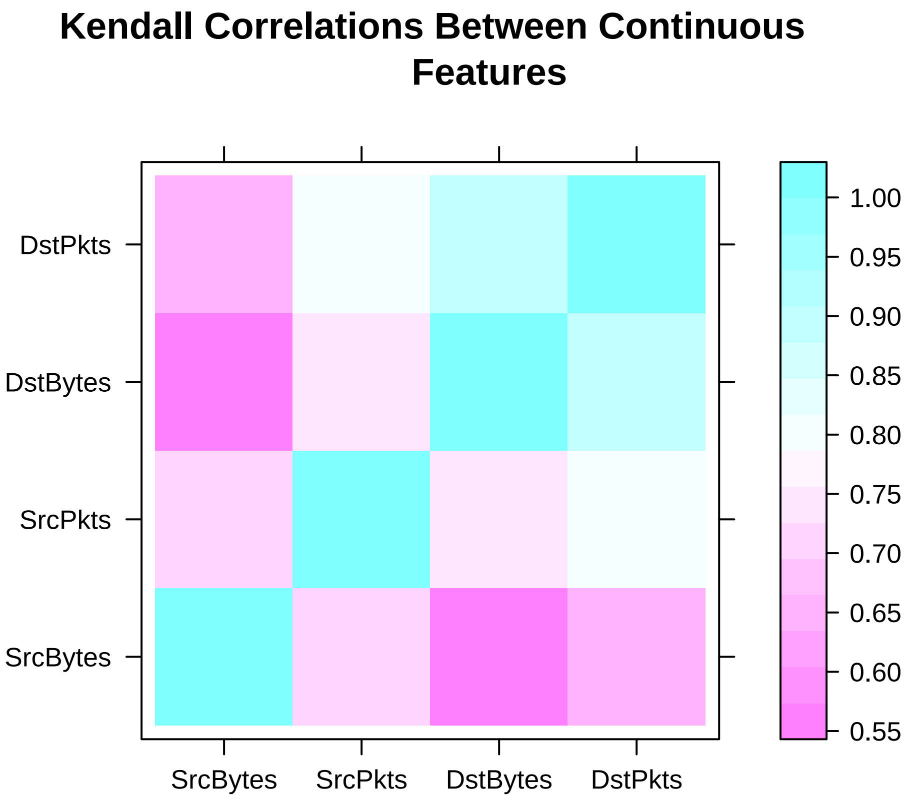

The strong correlations between the individual continuous features suggests imputing the tensor T all at once may yield closer estimates than the previous two techniques, which sliced the matrices. By imputing the tensor as a whole, techniques that include effects that capture the relationships between features can take advantage of possible collinearity between the features.

The following section describes the way techniques in the previous sections may be extended to full 3-dimensional tensor completion.

5.1 PARAFAC Decomposition

The PARAFAC decomposition expresses the tensor as:

$$T = \sum_{r=1}^{R} u_r \cdot v_r \cdot w_r$$

where r represents the rank approximation, $\cdot$ denotes the outer product of tensors, and $u \in \mathbb{R}^{m \times r}$, $v \in \mathbb{R}^{n \times r}$, and $w \in \mathbb{R}^{4 \times r}$. Each individual cell is expressed:

$$t_{ijk} = \sum_{r=1}^{R} u_{ri} \cdot v_{ri} \cdot w_{ri}$$

Applying this decomposition yields the objective

$$\min_{T'} \|T - T'\|$$

where

$$T' = \sum_{r=1}^{R} \lambda_r (u_r \cdot v_r \cdot w_r)$$

and λ_r is the regularization penalty.

5.2 Statistical Model

The following model is proposed:

$$t_{ijk} \sim N(\mu_{ijk}, \frac{\sigma_{ijk}^2}{s_{ijk}})$$

where μ_{ijk} is the sample mean, s_{ijk} is the sample size of observations, and σ_{ijk}^2 is the sample variance of observations for source port i, destination port j, and continuous feature k.

Substituting these values into the Gaussian probability density function yields the likelihood:

$$\frac{s_{ijk}}{\sigma_{ijk}^2} \sum (\bar{t}_{ijk} - \mu_{ijk})^2$$

Applying the PARAFAC decomposition, μ_{ijk} is re-expressed:

$$\mu_{ijk} = \sum_{r=1}^{R} a_{ir} b_{jr} c_{kr}$$

Vectorizing the inputs in the likelihood yields:

$$\sum_j \sum_k [\bar{t}_{ijk} - a_i^T (b_i \cdot c_k)] \frac{n_{ijk}}{\sigma_{ijk}^2}$$

where $a_i \in \mathbb{R}^{m \times r}$, $b_j \in \mathbb{R}^{n \times r}$, and $c_k \in \mathbb{R}4 \times r$. Summing across j and k in this case solves for the ith row slice of the tensor.

Conclusion

If we don't want Conclusion to have a chapter number next to it, we can add the `{-}` attribute.

More info

And here's some other random info: the first paragraph after a chapter title or section head *shouldn't be* indented, because indents are to tell the reader that you're starting a new paragraph. Since that's obvious after a chapter or section title, proper typesetting doesn't add an indent there.

Appendix A

Preliminary Data Investigation

A.1 Exploratory Data Analysis

A.1.1 Cleaning Predictors

```
     Flgs    SrcAddr      Sport    DstAddr      Dport    SrcPkts    DstPkts
 "factor"   "factor"   "factor"   "factor"   "factor" "integer" "integer"
 SrcBytes   DstBytes      State
"integer" "integer"   "factor"
```

This code casts the features to their corresponding class classifications (numeric and factor), and removes Proto, StartTime, and Diretion from the dataset.

A.1.2 Categorical Features: Unique Categories and Counts

A.1.3 Continuous Features: Distributions and Relationships

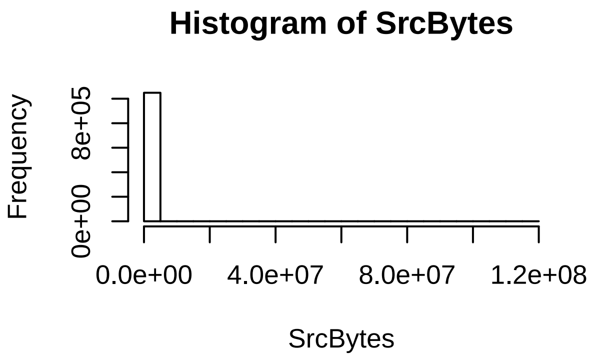

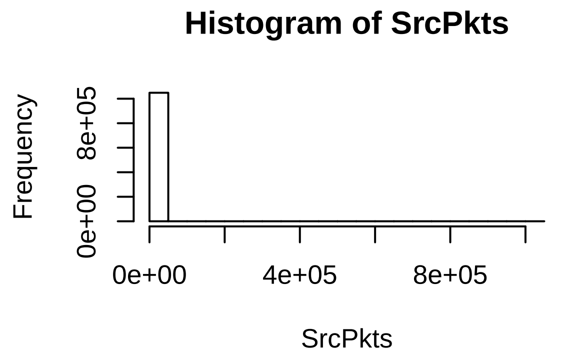

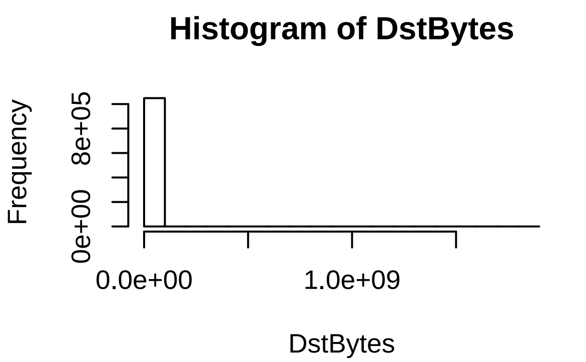

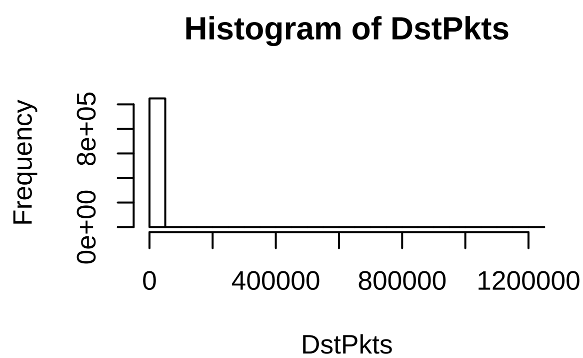


```
[1] 118257047 116615879 112673526 108933442 105793666  73376579  72839115
[8]  70001807  56206409  55359912

[1] 1008233 1000971  771590  492361  458603  437296  408530  407973
[9]  371976  371251

[1] 1850817751 1713055847 1690162763 1524781880 1491609296 1340922625
[7] 1304668214 1206594243 1163954979 1145323438

[1] 1239611 1223485 1219276 1004471  982931  942827  883354  795120
[9]  766776  754831
```

The histograms and the largest 10 values in each of the continuous variables show that there are a relatively few amount of large observations skewing the distributions. This explains the model summary containing means much larger than their medians. It's not possible to remove the large values as outliers because they may be scanner observations to detect. Also there is a high frequency (up to the first quartile) of destination bytes and packets that equal 0.

We will now try to investigate whether the largest continuous predictor values correspond to any particular addresses or ports.

```
            Flgs   SrcAddr Sport    DstAddr Dport SrcPkts DstPkts
282859  * s        1.0.12.1 18086  100.0.1.8 31743  208339  104886
282841  * s        1.0.12.1 18086  100.0.1.8 31743  204912   99688
282832  * s        1.0.12.1 18086  100.0.1.8 31743  198007   94621
282853  * s        1.0.12.1 18086  100.0.1.8 31743  191443   95892
282823  * s        1.0.12.1 18086  100.0.1.8 31743  186228   84342
724162  * *       100.0.4.9 37901 100.0.2.67    22 1008233 1239611
        SrcBytes   DstBytes State
282859 118257047    7514403   CON
282841 116615879    7146182   CON
282832 112673526    6801146   CON
282853 108933442    6857053   CON
282823 105793666    6048529   CON
724162  73376579 1713055847   CON
```

```
            Flgs   SrcAddr Sport    DstAddr Dport SrcPkts DstPkts
2162    * d       197.0.1.1 62030  100.0.1.1    80  371251 1219276
724162  * *       100.0.4.9 37901 100.0.2.67    22 1008233 1239611
724106  * *       100.0.4.9 37901 100.0.2.67    22 1000971 1223485
2212    * d       197.0.1.1 62034  100.0.1.1    80  280593 1004471
78245   * d         1.0.2.1 11210  100.0.1.2    80  158194  982931
2185    * d       197.0.1.1 62033  100.0.1.1    80  268402  883354
       SrcBytes   DstBytes State
2162   26430322 1850817751   CON
724162 73376579 1713055847   CON
724106 72839115 1690162763   CON
2212   20037592 1524781880   FIN
78245  11294111 1491609296   CON
2185   19137354 1340922625   FIN
```

Source Addresses tend to be repetitive for the largest max bytes/packets, while ports vary. The top 10 largest DstBytes all correspond to SrcAddr 197.0.1.1 and DstAddr 100.0.1.1. Also both max Src and Dst rows correspond to the “* s”" flag. The largest sizes of DstBytes tend to go to Dport 80, which is the port that expects to receive from a web client (http), while the largest SrcBytes go to 31743. The next section implements a systematic way for investigating the relationship between addresses and ports because simply looking at the max rows is difficult.

A.2 Transformations on the Data

A.2.1 Removing Quantiles

To get a better sense of the unskewed distribution, the below plots visualize the continuous features with the largest and smallest 10% of observations removed. The removed values will be readded to the dataset when investigating for anomalies.

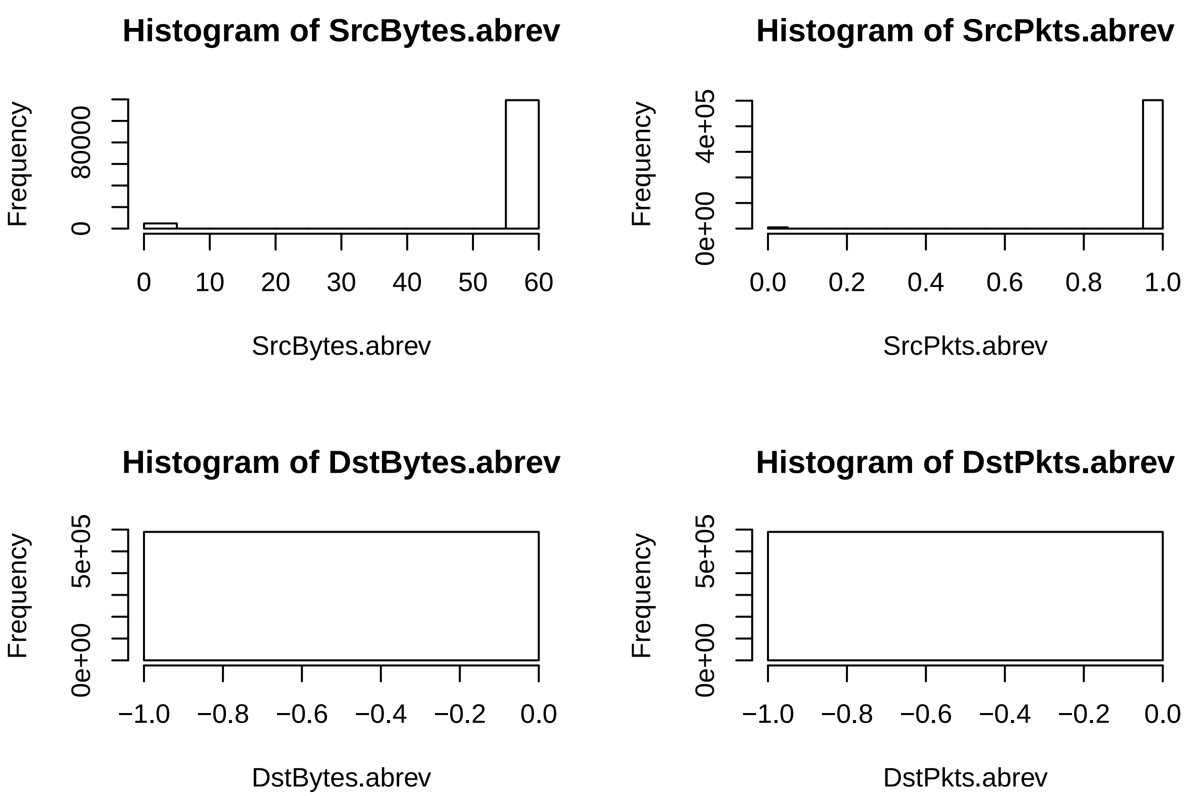

The continuous features are still unevenly distributed even with the 20% most extreme values removed.

A.2.2 Log Transformation

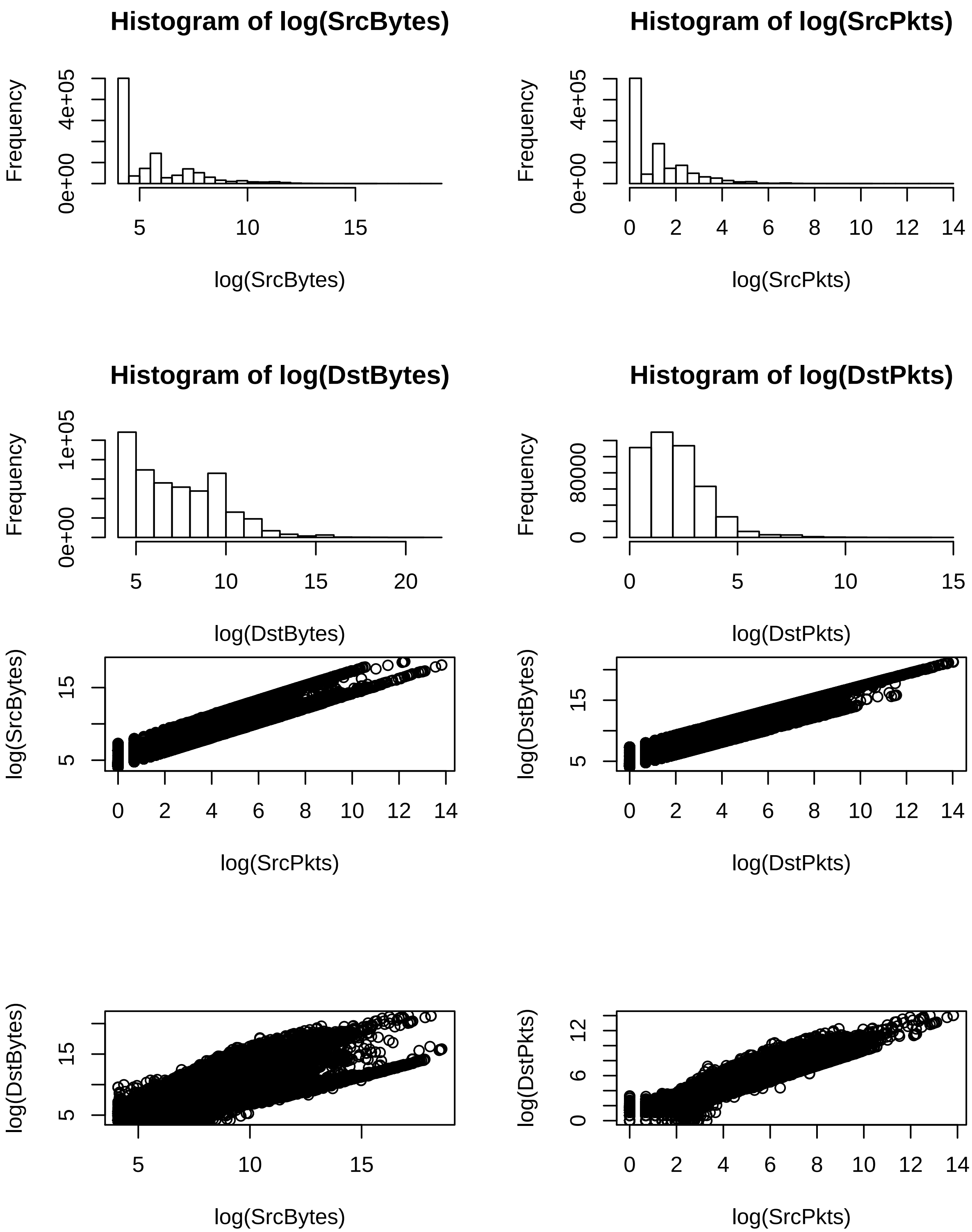

A log transformation for each of the continuous features outputs right-skewed histograms. Skewed features may affect the results of a kernel pca, so we consider other approaches for transformations.

A.2.3 Normal Scores Transformation

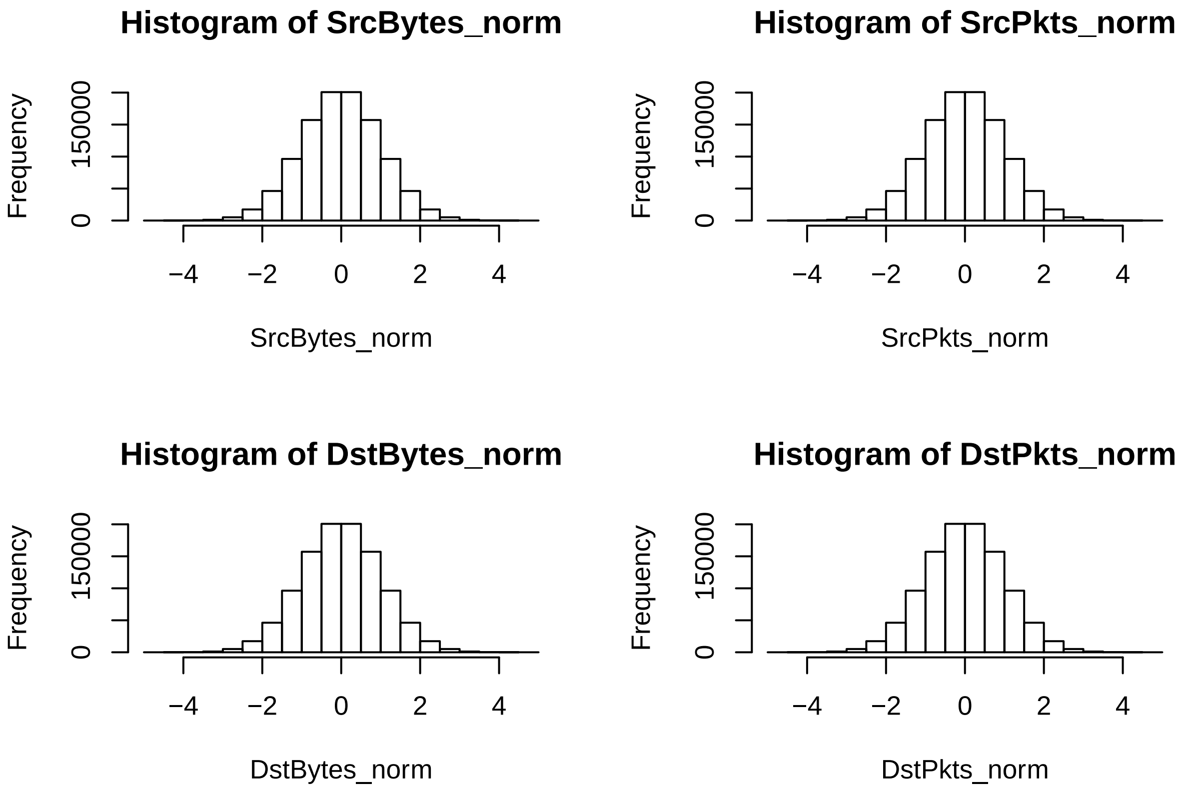

Finally, a normal scores transformation is applied to the dataset. The normal scores transformation reassigns each feature value so that it appears the overall data for that feature had arisen or been observed from a standard normal distribution. This transformation solves the issue of skewness-each value's histogram will now follow a standard gaussian density plot-, but it may cause issues with other analysis methods, particularly methods that are susceptible to ties in data.

A.3 Principal Component Analysis

Principal component analysis represents data in terms of its principal components rather than relying on traditional Cartesian axes. Principal components contain the underlying structure in data by representing the directions that contain the most variance. Each successive principal component is orthoganol to the previous, so the resulting vectors yields an uncorrelated orthogonal basis set. Because PCA is sensitive to relative scaling of variables, a normal scores transformation is applied before the algorithm is run.

A.3.1 Application

In this problem, Principal Component Anaylsis is applied to each source-destination port grouping of observed data to understand the underlying structure of the data partition's continuous features: source bytes and packets and destination bytes and packets. In particular the amount of variance explained by the generated principal components and their relative directions will signal whether specific trends in connection behavior occur at certain ports, and whether the size of each of the continuous features affects port behavior as well as the other features.

A.4 Implementation

A.4.1 Investigating Port Combinations

```
Sport: 32416    Dport: 9163
               PC1        PC2        PC3          PC4
SrcBytes 0.4113308 -0.7246604 -0.5528760  0.001575730
SrcPkts  0.5054262 -0.3234250  0.7999554  0.003459252
DstBytes 0.5357591  0.4327433 -0.1665939  0.705649994
DstPkts  0.5369483  0.4277813 -0.1632360 -0.708550377
Importance of components:
                          PC1    PC2     PC3     PC4
Standard deviation     1.7118 0.8991 0.51065 0.02309
Proportion of Variance 0.7326 0.2021 0.06519 0.00013
Cumulative Proportion  0.7326 0.9347 0.99987 1.00000
```

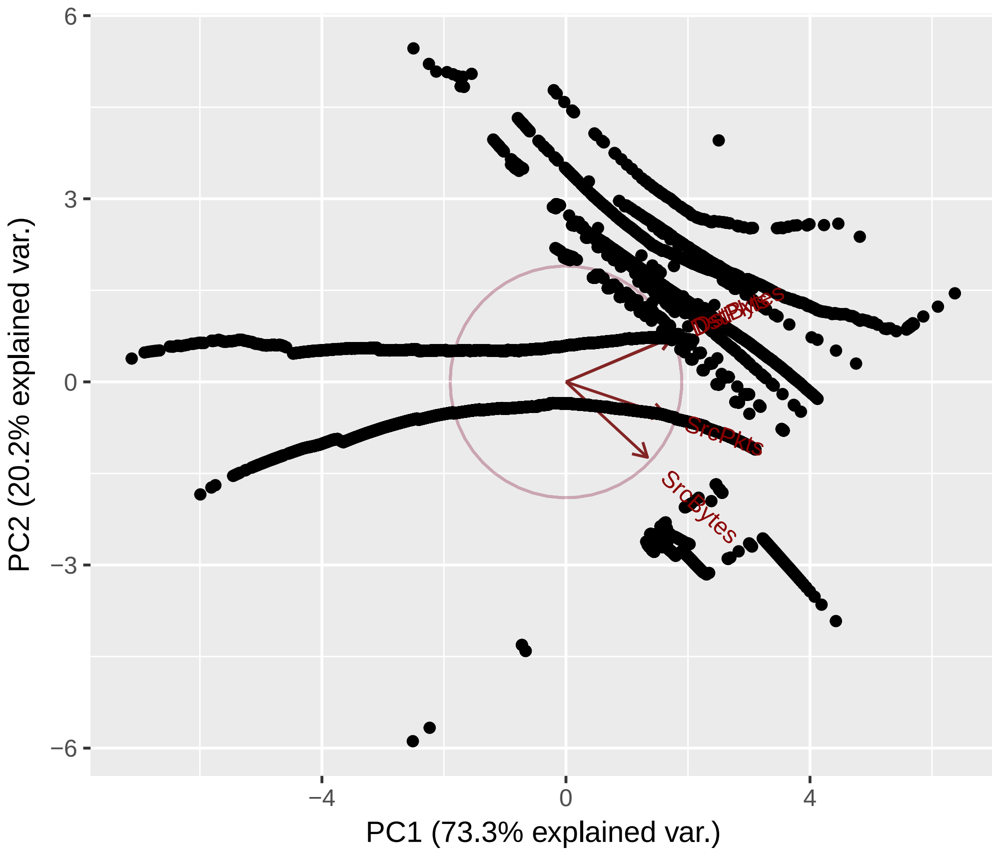


```
Sport: 4145     Dport: 9119
               PC1        PC2        PC3          PC4
SrcBytes 0.4333309  0.8902089 -0.1405308  0.001886624
SrcPkts  0.5213529 -0.1206221  0.8439979  0.036180840
DstBytes 0.5190742 -0.3165495 -0.3953966  0.688490995
DstPkts  0.5205549 -0.3045896 -0.3340362 -0.724339380
Importance of components:
                         PC1    PC2     PC3     PC4
Standard deviation     1.875 0.6538 0.23124 0.05551
Proportion of Variance 0.879 0.1069 0.01337 0.00077
Cumulative Proportion  0.879 0.9859 0.99923 1.00000
```

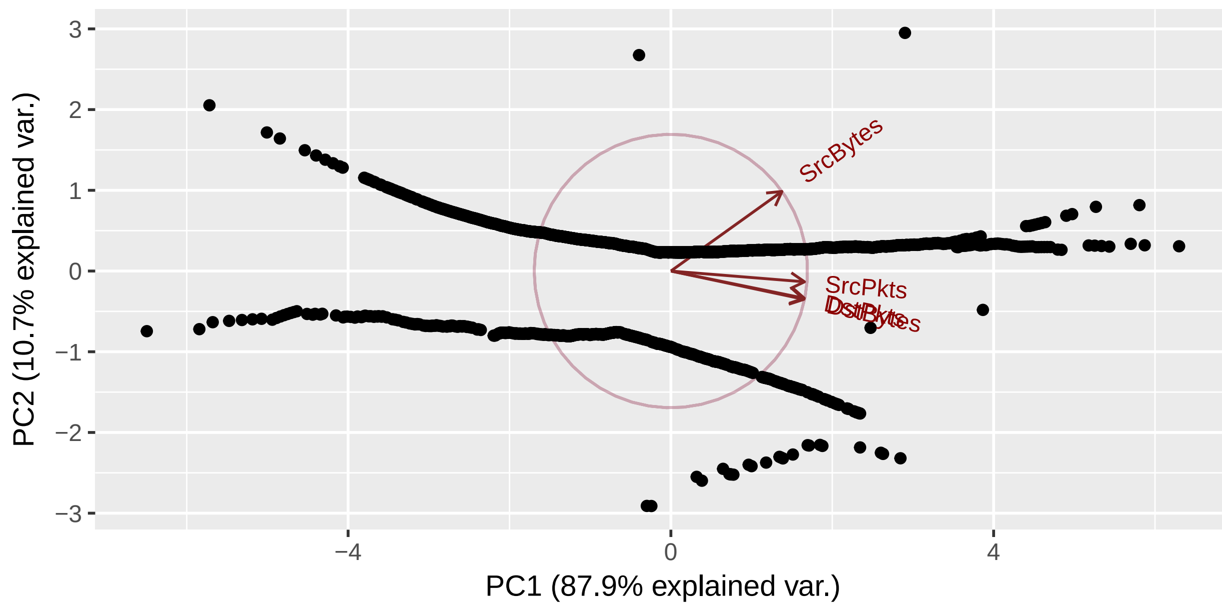


```
Sport: 19239    Dport: 9153
                PC1        PC2        PC3          PC4
SrcBytes 0.4400190  0.8125062 -0.3823817 -0.001104223
SrcPkts  0.5189497  0.1174251  0.8466938 -0.003489750
DstBytes 0.5179403 -0.4057384 -0.2640886 -0.705245607
DstPkts  0.5184712 -0.4017728 -0.2591352  0.708953621
Importance of components:
                          PC1    PC2     PC3     PC4
Standard deviation     1.8418 0.7037 0.33316 0.03695
Proportion of Variance 0.8481 0.1238 0.02775 0.00034
Cumulative Proportion  0.8481 0.9719 0.99966 1.00000
```

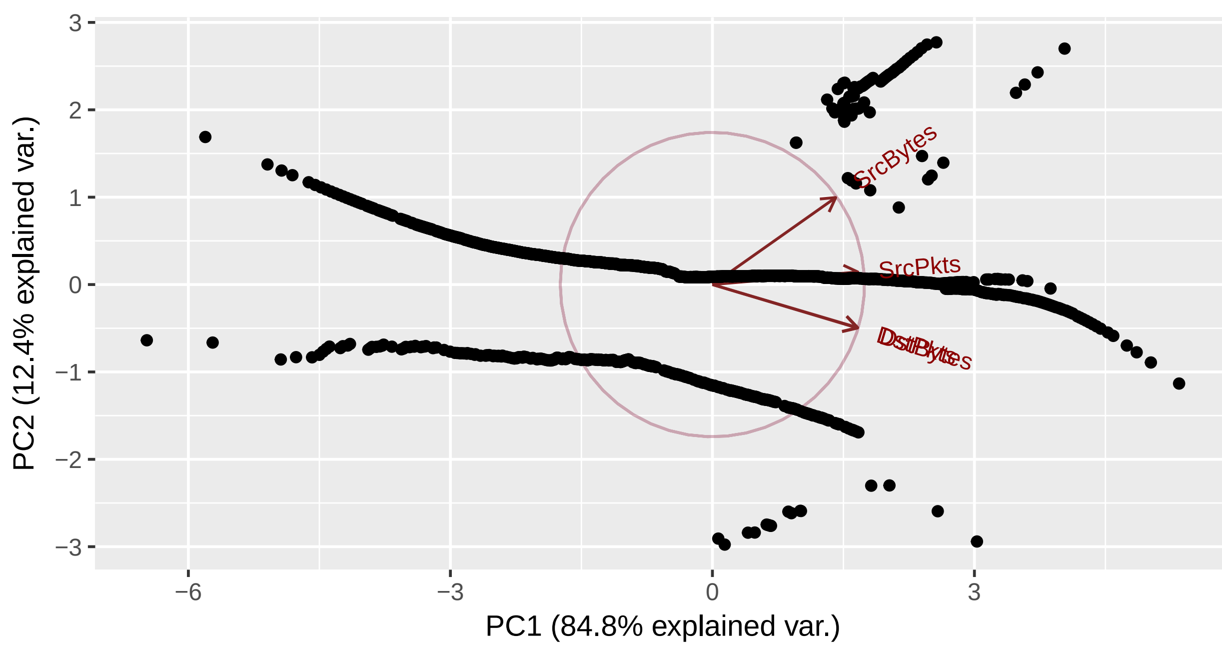

```
Sport: 4243     Dport: 27
                PC1        PC2        PC3          PC4
SrcBytes 0.3986539  0.8262979 -0.3978739  0.001762539
SrcPkts  0.5268775  0.1487193  0.8367993  0.007045781
DstBytes 0.5300998 -0.3876467 -0.2708012  0.703840168
DstPkts  0.5314785 -0.3805842 -0.2610173 -0.710321243
Importance of components:
                          PC1    PC2     PC3     PC4
Standard deviation     1.7727 0.8343 0.40033 0.03406
Proportion of Variance 0.7856 0.1740 0.04007 0.00029
Cumulative Proportion  0.7856 0.9596 0.99971 1.00000
```

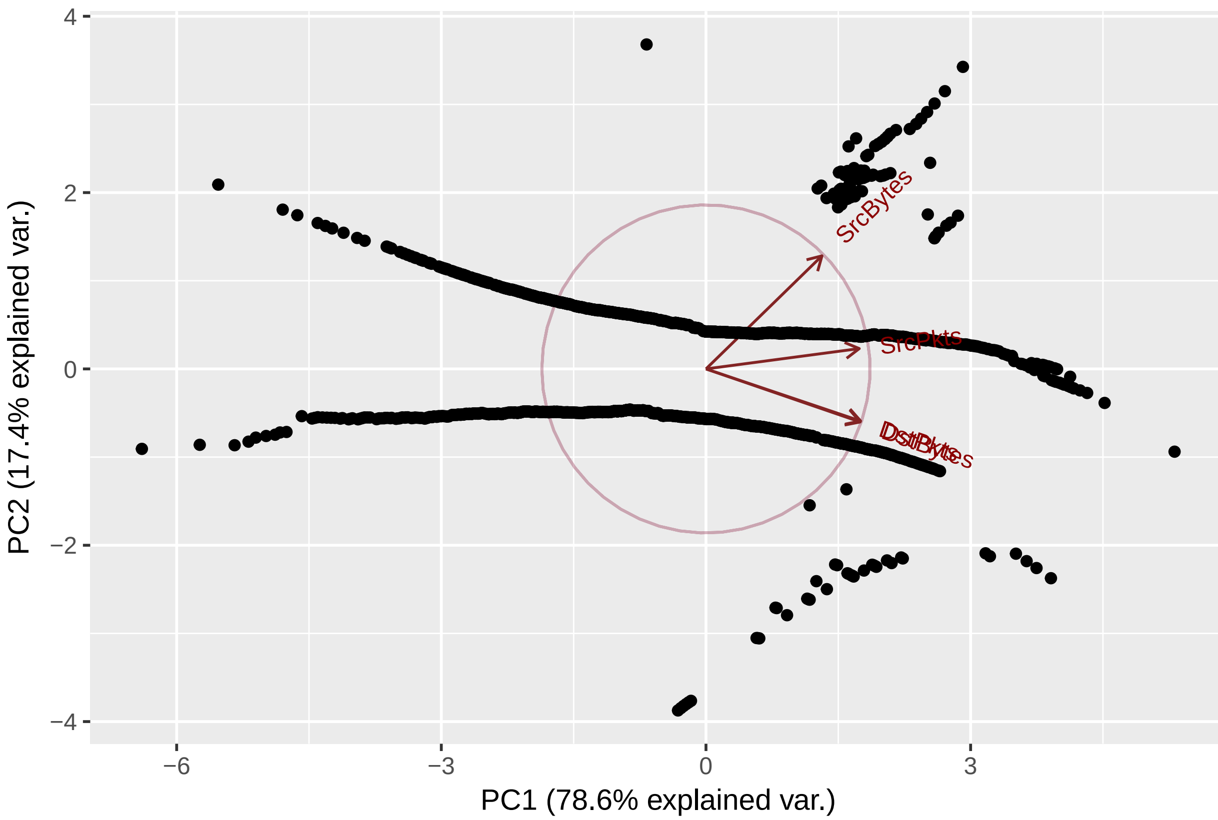


```
Sport: 4243     Dport: 10290
                 PC1         PC2        PC3          PC4
SrcBytes -0.4146349  0.86007431 -0.2972268 -0.002501828
SrcPkts  -0.5225073  0.04229265  0.8514240 -0.016572825
DstBytes -0.5257892 -0.36545098 -0.3181251 -0.699133556
DstPkts  -0.5278350 -0.35345310 -0.2924547  0.714794623
Importance of components:
                          PC1    PC2     PC3     PC4
Standard deviation     1.8125 0.7560 0.37528 0.05022
Proportion of Variance 0.8213 0.1429 0.03521 0.00063
Cumulative Proportion  0.8213 0.9642 0.99937 1.00000
```

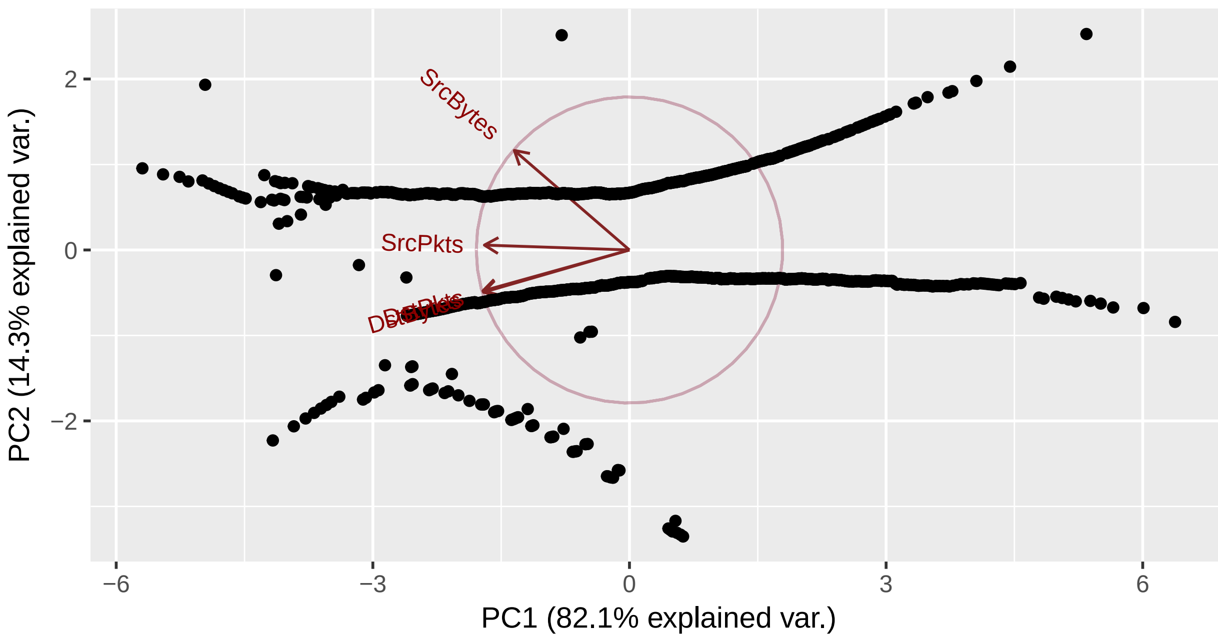

A.4.2 Interpretation

In general the first two principal components explained most of the variance (~90%) for each of the port combinations. The scatterplots of the principal components show clear horizontal patterns in the 2nd principal component. This similar behavior, mirrored throughout the top 10 most frequent ports, may be caused by the high frequency of zeroes in the dataset. Recall, the first quartile of observations for destination bytes and packets were all 0. This high frequency of the same value (0) yields ties when performing the normal scores transformation applied to the data, which may also cause the horizontal behavior exhibited in every principal component analysis.

References

Angel, E. (2000). *Interactive computer graphics : A top-down approach with opengl*. Boston, MA: Addison Wesley Longman.

Angel, E. (2001a). *Batch-file computer graphics : A bottom-up approach with quicktime*. Boston, MA: Wesley Addison Longman.

Angel, E. (2001b). *Test second book by angel*. Boston, MA: Wesley Addison Longman.